Performance of Power-Controlled Wideband Terrestrial Digital Communication

Andrew J. Viterbi, *Fellow, IEEE,* Audrey M. Viterbi, *Member, IEEE,* and Ephraim Zehavi, *Member, IEEE*

***Abstract*—Performance of a wideband multipath-fading terrestrial digital coded communication system is treated. The analysis has applications to a cellular system employing direct sequence spread spectrum CDMA with M-ary orthogonal modulation on the many-to-one reverse (user-to-base station) link. For these links, power control of each multiple access user by the cell base station is a critically important feature. This is implemented by measuring the power received at the base station for each user and sending a command to either raise or lower reverse link transmitted power by a fixed amount. Assuming perfect interleaving, the effect of the power-control accuracy on the system performance is assessed.**

I. Introduction

In terrestrial wireless transmission for cellular, mobile, and personal communication services, the channel is subject to time varying carrier amplitude and phase. While, in narrowband channels, the multipath propagation causes carrier signal cancellation (by equal-delay opposite phase paths) and consequent deep fades, wideband signals suffer from much shallower fading with multiple paths appearing as interference often separated in time. With spread spectrum code division multiple access (CDMA) techniques, the multiple paths can be demodulated individually by a "RAKE-type" receiver and combined prior to a decision, thus minimizing interference and mitigating fading further. Finally, in systems employing multiple base stations or cell sites, generally referred to as cellular systems, power control, which is desirable or required to control other-user interference, also serves to mitigate shadowing when the control is sufficiently rapid.

This paper deals with the many-to-one reverse links from multiple access users to a cellular base station. Assuming the classical multipath-fading model, for which there is ample experimental evidence for wideband signals [1], [2], and a conventional direct-sequence spread-spectrum waveform, error performance is determined for a convolutionally coded M-ary orthogonal modulation with noncoherent envelope-detector matched filter demodulation. Effects of shadowing, typically modeled as log-normally distributed multiplicative interference, is mitigated through the use of power control whose performance is also analyzed.

Paper approved by the Past Editor-in-Chief of the IEEE Communications Society. Manuscript received May 6, 1991; revised December 11, 1991.

A. J. Viterbi and A. M. Viterbi are with Qualcomm Inc., San Diego, CA 92121-1617

E. Zehavi was with Technion-Israel Institute of Technology, Department of Electrical Engineering, Technion City, Haifa 32000, Israel. He is currently with Quelcomm, Incorporated.

IEEE Log Number 9209478.

However, the main purpose of power control is to maintain all users' signal energy received at the base station nearly equal in the spread spectrum which is shared in common. Since each user's signal appears as interference to all other users, the total capacity of the system [3] depends on tight power control. Another benefit is that each user transmits only as much energy as is required to maintain a given level of error performance; hence, its overall transmitted energy is kept at a minimum, thus prolonging battery life in portable transmitters.

II. Characterization of Spread Spectrum CDMA Communication System and Multipath- Fading Channel

The end-to-end communication system block diagram (as shown in Fig. 1) can be subdivided into five components:

a) the encoder-interleaver-waveform generator;
b) the spreading processors, D/A converters (impulse modulation), shaping filters, upconverter, and power amplifier;
c) the multipath channel;
d) the downconverter, matched filter, despreader, A/D converter (sampler); and
e) The multiple demodulator-deinterleaver-soft decision decoder.

The spread spectrum modulator (b) is as described in [4]. The shaping filters are typically finite impulse response (FIR) digital filters to which the receiver filters are matched (mirror image impulse response and conjugate transfer function). Their purpose is to contain the transmitted energy in the allocated wideband spectrum of bandwidth W, which is the inverse of T_c, the spreading sequence switching time, generally called the chip time. The power amplifier has its output power controlled digitally as described in a later section.

To streamline the diagram, all two-component (I and Q) signals are represented as complex quantities and the corresponding (two-component) branches are shown as double lines. Thus, the quadrature spreading by multiplication by the independent pseudorandom (PN) sequences, the two-branch baseband filters $H(f)$, and the upconverting carrier multipliers are all treated in this way.

The classical model for multipath is a delay line, with delays corresponding to discernable paths each scaled by a complex random variable with Rayleigh distributed amplitude and uniformly distributed phase. The incremental delays $\tau_k - \tau_{k-1}$ must be larger than T_c, the inverse of the spread spectrum bandwidth W, in order for the multipath components to be distinguishable (those that are not distinguishable combine

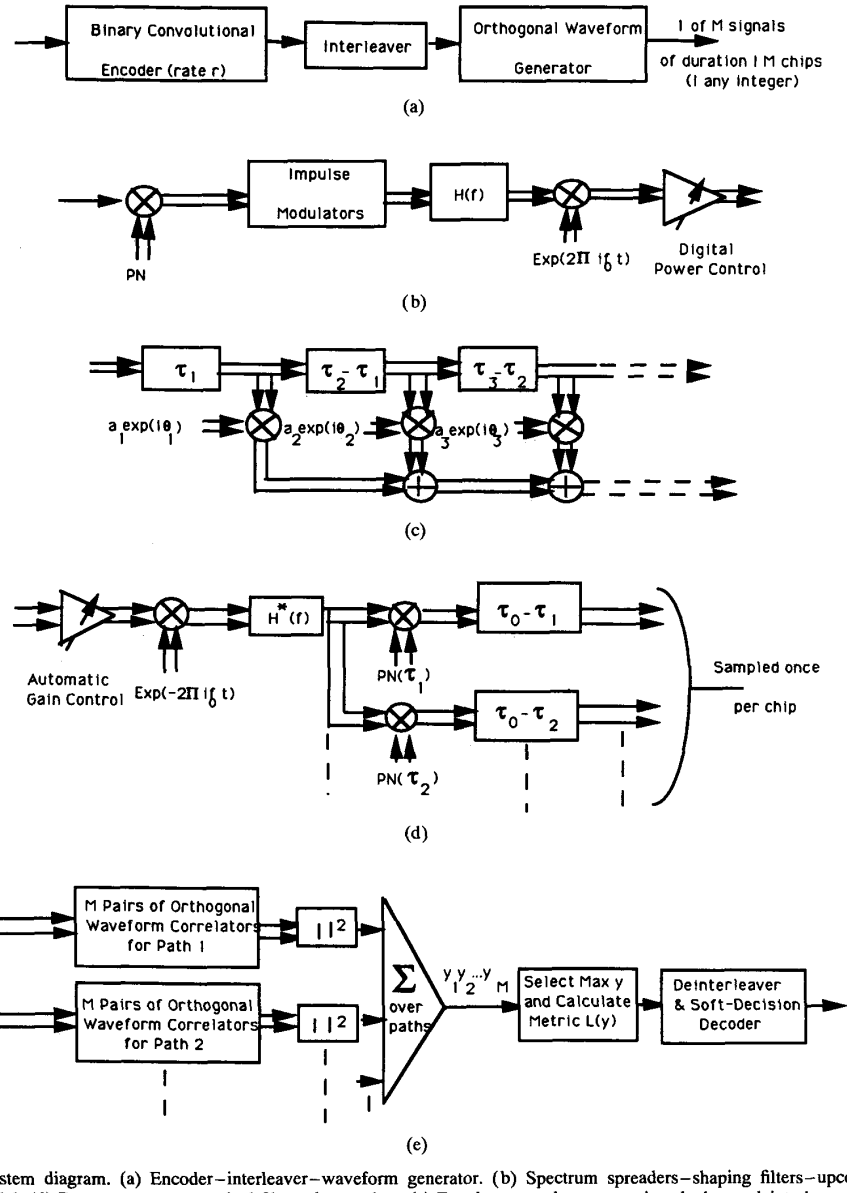

Fig. 1. Overall link system diagram. (a) Encoder–interleaver–waveform generator. (b) Spectrum spreaders–shaping filters–upconverter. (c) Multipath channel model. (d) Downconverter–matched filter–despreaders. (e) Envelope correlators–metric calculator–deinterleaver–decoder.

randomly, thereby giving rise to the Rayleigh distributed amplitudes and uniform phases of the scale factors). Thus, the overall complex transfer function of the m-component multipath channel is

$$\sum_{k=1}^{m} a_k \exp(i\Theta - 2\Pi i f_0 \tau_k).$$

It is assumed that the distinguishable individual path delays can be measured. Of course, in a mobile or otherwise changing propagation environment, these delays must be tracked; also, some will disappear after time while new ones appear. However, these will vary slowly compared to the bit rate, and hence can be accurately estimated and tracked. Amplitudes and phases, on the other hand, will vary more rapidly and are not estimated, but rather are taken to be independent, identically distributed variables constant at least over each transmitted orthogonal waveform.

The optimum receiver for such a channel [5] is as shown in Fig. 1(d). After downconversion and matched filtering by $H^*(f)$, the received signal is despread independently for each multipath component by multiplying by the quadrature spreading sequences delayed by an amount equal to the delay of that multipath component. Thus, the demodulator is effectively replicated m-fold, once for each significant multipath delay. To line up the multipath components after despreading, each must be delayed by a complementary amount $\tau_0 - \tau_k$, where

τ_0 is greater than any of the path delays. This is generally called a "RAKE" receiver [6]. Sampling and A/D conversion can be performed after the despreading or before, provided in the latter case that the received signal is oversampled to the accuracy of the delay measurements.

The form of the demodulator-decoder [Fig. 1(e)] depends on the choice of coder-modulator[1] [Fig. 1(a)]. Since amplitudes and phases can be assumed to remain essentially constant over a few bit times, this suggests the use of M-ary orthogonal waveforms whose time duration is no greater than the duration over which the fading amplitudes and phases remain virtually unchanged. Using binary waveforms only, such M-ary orthogonal waveforms can be generated using Hadamard or Walsh functions [4] whose duration is M chip times of the PN sequence, or any multiple thereof. Thus, if the input bit rate is R, and the code rate of the preceding encoder is r, using M chip times per orthogonal waveform implies that the bandwidth would be $W = 1/T_c = RM/(\log_2 M)r$. The bandwidth can be expanded by any multiple of this quantity by making each symbol of the Hadamard–Walsh function be I chips long. Thus, the ratio of bandwidth-to-bit rate, usually called the processing gain, is

$$W/R = IM/(\log_2 M)r, \qquad \text{where } I \text{ is any integer}.$$

As a specific example, with $M = 64$ orthogonal waveforms and $r = 1/3$, W/R can be made any multiple of 32; with $I = 4$, the processing gain is 128 or 21 dB.

III. Signal Statistics, Metric Calculation, and Soft-Decision Decoder Performance

The output of each envelope-detector correlator pair in Fig. 1(e) is a nonnegative random variable z with probability density function

$$P_C^{(z)} = e^{-z/(S+1)},$$

if the correlator corresponds to the correct signal sent

$$P_I^{(z)} = e^{-z}, \qquad \text{if the correlator corresponds to one of the } M-1 \text{ other (incorrect) signals}$$

where it is assumed that automatic gain control (AGC) has normalized the noise variance to unity, and S is the normalized mean received energy per path. Thus, if $\overline{E}$ is the total received energy per orthogonal waveform summed over all m equal average energy paths, and N_0 is the additive noise density, including other-user spread signals [3], [4], then

$$S = (\overline{E}/N_0)/m.$$

Assuming, as we have, that all m paths are mutually independent, the sum of all m paths for the correct signal correlator $y = \sum_{k=1}^{m} z_k$ has probability density which is the m-fold convolution of that for each path, $p_C(z)$,

$$f_C^{(m)}(y) = \frac{y^{m-1}e^{-y/(S+1)}}{(m-1)!\,(S+1)^m}. \tag{1a}$$

For each of the incorrect signal correlators, it is the m-fold convolution of $p_I(z)$

$$f_I^m(y) = \frac{y^{m-1}e^{-y}}{(m-1)!}. \tag{1b}$$

For the sake of comparison, we also consider the case of only one *unfaded* path, for which it is well known that, for fixed signal energy E,

$$f_C^U(y) = e^{-(y+E/N_0)} I_0\left(2\sqrt{(E/N_0)y}\right) \tag{2a}$$

$$f_I^U(y) = e^{-y}. \tag{2b}$$

The probability that an error is made by the maximum likelihood detector, which results when one of the $M-1$ random variables y_j corresponding to an incorrect signal exceeds that for the correct signal, as derived from (1) or (2), is well known [7], [8]. However, the soft decision decoder operates not only on the decision of which y_j is maximum, but also on their relative magnitudes. To reduce complexity (of both implementation and analysis), we consider only the magnitude of the maximum correlator output

$$y = \text{Max } y_j.$$

The input to the soft decision decoder is this value along with the index of y, which is a binary sequence of length $\log_2 M$ representing the (hard) decision symbols. Note that upon deinterleaving, the value of y (soft decision) must be attached to each (deinterleaved hard decision) symbol of the index, which shall be denoted x.

The optimum choice of binary metrics, based only on the value of y and any one of the binary symbols x to which it pertains, is obtained from the two joint likelihood functions of y and x, given that it did and did not correspond to what was sent. These are, respectively,

$$p(y,x|x) = f_C(y)F_I(y)^{M-1} + (M/2-1)f_I(y)F_C(y)F_I^{M-2}(y), \tag{3a}$$

$$p(y,x|\overline{x}) = (M/2)f_I(y)F_C(y)F_I^{M-2}(y) \tag{3b}$$

where $x = 0$ or 1 and $\overline{x}$ is its complement,[2] and $f_C(y)$ and $f_I(y)$ are given by (1) or (2). $F_C(y)$ and $F_I(y)$ are the corresponding distribution functions, their indefinite integrals. Note that $f_C(y)$ and $F_C(y)$ depend also on $\overline{E}$ and E in the faded and unfaded cases, respectively.

The expression (3b) follows from the fact that the density function of the largest of $(M-1)$ incorrect signal measured

[1] Use of a binary convolutional encoder with interleaving prior to M-ary orthogonal waveform selection is superior to encoding the M-ary orthogonal waveforms directly without binary symbol interleaving, as demonstrated in Appendix II.

[2] Alternately, if we take x to be $+1$ or -1 (or any multiple thereof) and $\overline{x}$ its negative, then the joint densities could be denoted as the four one-dimensional densities $p(\pm y|x = \pm 1)$, where $y > 0$.

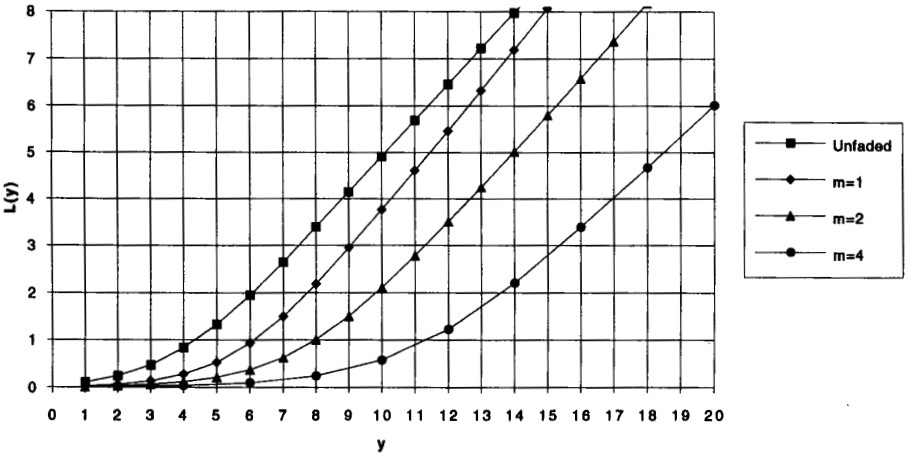

Fig. 2. Log-likelihood ratio (E/N_o = 10 dB; M = 64).

energies, when it is greater than the correct signal measured energy, is $(M-1)f_I(y)F_I^{M-2}(y)F_C(y)$, and conditioned on this, a symbol error ($\overline{x}$ mistaken for x) occurs with probability $M/[2(M-1)]$.

The expression (3a) follows from the fact that a symbol can be correct in either of two disjoint events: if the correct decision is made, in which case the correct signal energy is greatest with density $f_C(y)F_I(y)^{M-1}$; or if the incorrect decision is made (with density as given above) but the binary symbol is nonetheless correct, which occurs with probability $(M/2-1)/(M-1)$.

Given the observable y with density function given by (3a) and (3b), the optimum metric is the log-likelihood function, formed from the ratio of (3a) and (3b).

$$\exp[L(y)] \triangleq \frac{p(y,x|x)}{p(y,x|\overline{x})} = \left(1-\frac{2}{M}\right)+\frac{2}{M}\,\frac{f_C(y)F_I(y)}{f_I(y)F_C(y)}. \tag{4}$$

$L(y)$ is plotted in Fig. 2 for $M=64$ and $E/N_0 = 10$ dB for the unfaded signal case, and for the m-path fading case for $m=1,2$ and 4 with $\overline{E}/N_0 = 10$ dB.

Using this ideal soft metric, which requires knowledge of E in the unfaded case and $S=(\overline{E}/N_0)/m$ in the faded cases, the performance parameter Z for a soft decision decoder (see Appendix I) then becomes

$$\begin{aligned} Z &= 2\int_0^\infty \sqrt{p(y,x|x)p(y,x|\overline{x})}\,dy \\ &= 2\int_0^\infty p(y,x|\overline{x})\sqrt{\exp[L(y)]}\,dy \\ &= M\int_0^\infty f_I(y)F_C(y)F_I^{M-2}(y) \\ &\quad\cdot\left[\left(1-\frac{2}{M}\right)+\frac{2}{M}\,\frac{f_C(y)F_I(y)}{f_I(y)F_C(y)}\right]^{1/2} dy. \end{aligned} \tag{5}$$

Using (1) or (2) and (5), for a range of E/N_0 and $\overline{E}/N_0 = mS$, Z was integrated numerically for the unfaded case and for multipath-fading with $m=1,2$, and 4.

From Z, according to Appendix I, we obtain the following parametric relationship between required $\overline{E}/N_0$ and code rate r for any $\alpha = r_0/r > 1$.

$$\frac{1/r}{\alpha} = 1/r_0 = \frac{1}{1-\log_2(1+Z)} \tag{6}$$

$$\begin{aligned} \frac{\overline{E}_b/N_0}{\alpha} &= \frac{\overline{E}/N_0}{\alpha r\log_2 M} = \frac{\overline{E}/N_0}{r_0\log_2 M} \\ &= \frac{\overline{E}/N_0}{[1-\log_2(1+Z)]\log_2 M}, \\ &\quad \text{where } \overline{E}/N_0 = E/N_0, \text{unfaded} \\ &\quad \text{and } \overline{E}/N_0 = mS, \text{ multipath-fading}. \end{aligned} \tag{7}$$

This relation is plotted as solid curves in Fig. 3 for the unfaded cases and for fading with $m=1,2$, and 4 multipath components, and for $M=64$ orthogonal waveforms.

Since α is established from the error probability requirement (α = 0.6 dB and 0.8 dB for the rate 1/2 and rate 1/3 codes, respectively[3]), required $\overline{E}_b/N_0$ can be obtained from Fig. 3 by backing off α (in dB) from $1/r$ (in dB), and, from this finding the corresponding $(\overline{E}_b/N_0)/\alpha$ (in dB) and finally adding α (in dB). With the α values noted, this represents E_b/N_0 requirements of 4.9 dB and 5.2 dB for the unfaded case at rate 1/2 and 1/3, respectively. For the three faded cases at rate 1/2, $\overline{E}_b/N_0$ requirements range from 7.0 dB to 7.9 dB; at rate 1/3, $\overline{E}_b/N_0$ required ranges from 7.1 dB to 7.5 dB. Hence, rate 1/3 is the better choice globally.

IV. Performance Bounds for Integer Metrics

While the optimum metric is the log-likelihood function $L(y)$ given in (4) and shown in Fig. 2 for various fading and unfaded channels, practical implementation requires quantization of the maximum energy y. Scaling any $L(y)$ by an arbitrary amount does not affect decoder performance in any way, although quantization obviously does. A reasonable approximation based on an 8-level quantizer, which uses integer

[3] For error probabilities of approximately 0.01 for 200-bit frames.

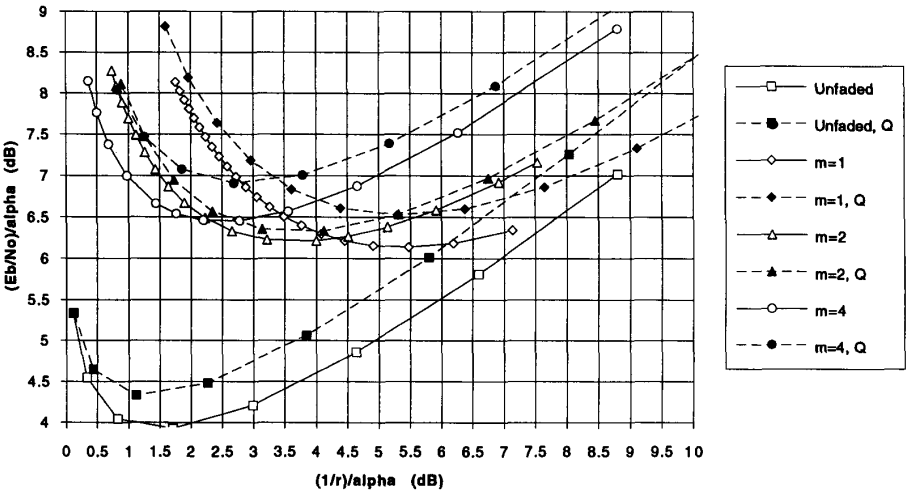

Fig. 3. Performance bound for m-path fading propagation ($M = 64$).

representative values, utilizes the quantization thresholds at values of y : $\theta_0 = 0$, $\theta_1 = 7$, $\theta_2 = 9$, $\theta_3 = 11$, $\theta_4 = 12$, $\theta_5 = 13.5$, $\theta_6 = 15$, $\theta_7 = 16.5$, $\theta_8 = \infty$. This best approximates the metric $L(y)$ for the two-path Rayleigh fading case but, as we shall see, performance is in no case degraded by more than 0.5 dB.

Quantization converts the continuous binary-input channel described by $p(y, x|x)$ and $p(y, x|\overline{x})$, into a binary-input discrete symmetric-output channel with transition probabilities

$$P_{+k} = \int_{\theta_{k-1}}^{\theta_k} p(y, x|x)\, dy, \qquad k = 1, 2, \cdots, 8, \tag{8a}$$

$$P_{-k} = \int_{\theta_{k-1}}^{\theta_k} p(y, x|\overline{x})\, dy, \qquad k = 1, 2, \cdots, 8. \tag{8b}$$

Note that, in this formulation, hard decisions correspond to a single level ($k = 1$) with plus and minus unity metric and $\theta_0 = 0$, $\theta_1 = \infty$.

Substituting (3a) and (3b) into (8a) and (8b) and integrating by parts yields

$$P_{+k} = \frac{M/2 - 1}{M - 1} F_C(y) F_I^{M-1}(y)\Big|_{\theta_{k-1}}^{\theta_k} + \frac{M/2}{M - 1} \int_{\theta_{k-1}}^{\theta_k} f_C(y) F_I^{M-1}(y)\, dy \tag{9a}$$

$$P_{-k} = \frac{M/2}{M - 1} F_C(y) F_I^{M-1}(y)\Big|_{\theta_{k-1}}^{\theta_k} - \frac{M/2}{M - 1} \int_{\theta_{k-1}}^{\theta_k} f_C(y) F_I^{M-1}(y)\, dy. \tag{9b}$$

Coded performance with an ideal interleaver can now be evaluated based on the Chernoff bound for this quantized channel.

$$Z = \operatorname*{Min}_{s>0} E\left(e^{-s\hat{y}}\right)$$

where $\hat{y}$ is the quantized energy metric which takes on integer value $\pm(k - 1)$, where $k = 1, 2, \cdots, 8$. Thus, letting $w = e^{-s}$ $(w < 1)$,

$$Z = \operatorname*{Min}_{w<1} E\left(w^{\hat{y}}\right) = \operatorname*{Min}_{w<1} \sum_{k=1}^{8} \left(P_k w^{k-1} + P_{-k} w^{-(k-1)}\right) \tag{10}$$

for the soft quantizer[4] considered here.

As in the ideal unquantized case, $\overline{E}_b/N_0$ and r are related by (6) and (7) through Z, given by (10) in this case. The results are plotted as dotted lines in Fig. 3, where they are seen to degrade performance for the unquantized cases by never more than 0.5 dB.

V. Power Control With Ideal Interleaving and Lognormal Shadowing

Given the integer metric demodulator described in the last section, a natural method of providing power control for a channel, in which the average energy varies slowly, is to take the quantized maximum M-ary signal demodulator energies (as before normalized by AGC so that the average noise-only energy is unity), sum them over N signal periods, and compare these with a threshold. If the threshold is exceeded, a command is sent via a (low data rate) command channel from the cell base station to lower the energy a given amount in decibels and otherwise to raise it by the same amount. It is assumed that the command to raise or lower is sent uncoded so as to minimize its delay, and hence is subject to a higher error rate.

Thus, assuming a given average energy-to-noise level $\overline{E}$ and summing N successive quantized normalized maximum energies

$$Y = \sum_{n=1}^{N} \hat{y}(n)$$

[4] Note that for hard decisions (two levels with metrics ± 1) $Z = 2\sqrt{P_1 P_{-1}}$ with $\Theta_0 = 0$ and $\Theta_1 = \infty$.

and comparing with the threshold ϕ, results in a probability of sending a command to lower energy equal to

$$P_d = \Pr\left(\sum_{n=1}^{N} \hat{y}(n) > \phi\right). \tag{11}$$

Each term of the sum is a discrete random variable which takes on the quantizer's representative values, which, as above, are taken to be the eight integers $k-1=0$ through 7, which occur with probability

$$Q_k = \Pr(\theta_{k-1} \le \hat{y} < \theta_k) \qquad k = 1, 2, \cdots, 8 \tag{12}$$

where θ_k are the quantization thresholds. These are readily determined to be the unconditioned probabilities

$$Q_k = F_C(y) F_I^{M-1}(y)\big|_{\theta_{k-1}}^{\theta_k} \tag{13}$$

which are thus related to the transition (conditional) probabilities of (9) by

$$Q_k = P_{+k} + P_{-k}.$$

Now letting

$$Q(w) \triangleq \sum_{k=1}^{8} Q_k w^{k-1} \tag{14}$$

be the moment generating function of each $\hat{y}(n)$, the moment generating function of the sum $Y = \sum_{n=1}^{N} \hat{y}(n)$ is

$$[Q(w)]^N = Q_1^N w^0 + \cdots + Q_8^N w^{7N}.$$

Finally, to compute (11), we must sum all the coefficients of this polynomial for terms whose powers have integer value greater than ϕ. We denote this as

$$P_d = \left\{[Q(w)]^N\right\}_{\phi^+}. \tag{15}$$

Clearly, the probability of sending a command to increase power is

$$P_u = 1 - P_d. \tag{16}$$

Finally, as noted, errors can occur in the command link with probability γ. Since this is independent of the above expressions, the overall probability that the command to increase power is received by the transmitter (correctly or incorrectly) is

$$P_U = (1-\gamma)P_u + \gamma P_d = (1-\gamma) - (1-2\gamma)P_d, \tag{17}$$

while the command to decrease power is received by the transmitter with probability

$$P_D = (1-\gamma)P_d + \gamma P_u = \gamma + (1-2\gamma)P_d. \tag{18}$$

Thus, P_U and P_D can be determined from (13), (14), and (15). Throughout the following, the erroneous command probability γ will be taken equal to 0.05.

As assumed above, power control commands are determined on a measurement interval comprising N contiguous M-ary transmissions, over which the average received signal energy is taken to be constant. While it would be desirable to take action immediately, the processing delay (plus the generally small propagation delay) introduces a lag (or latency) in the control loop of one measurement interval (N M-ary symbol transmissions). Now suppose that at the rth measurement interval, the transmitted signal energy is T_r while the average received signal energy is

$$\overline{E}_r = T_r - L_r \tag{19}$$

where L_r is the channel propagation loss, all quantities being in decibels. Now because of the control and the one measurement interval delay, the transmitted energy at the $(r+1)$th interval is

$$T_{r+1} = T_r + C(\overline{E}_{r-1})\Delta \tag{20}$$

where Δ is the fixed increment of increase or decrease in decibels and

$$C(\overline{E}_{r-1}) = \begin{cases} +1 & \text{if an up command was received,} \\ & \text{with probability } P_U \\ -1 & \text{if a down command was received,} \\ & \text{with probability } P_D \end{cases} \tag{21}$$

where P_U and P_D are given by (17) and (18), which in turn depend on $\overline{E}$ through (13)–(15).

Further combining (19), (20), and (21) yields

$$\overline{E}_{r+1} = \overline{E}_r + C(\overline{E}_{r-1})\Delta - (L_{r+1} - L_r). \tag{22}$$

We assume that the propagation loss, including distance and fading induced losses, exhibits independent random increments (as a Brownian motion). This would lead to unbounded variance if the control were not present. On the other hand, for a mobile user who may travel rapidly over a variety of terrains and is subject to blockages, the independent increment model is justifiable. In any case, with the control present, the received energy's variance is always finite.

The nonlinear difference equation (22) is reminiscent of similar differential equations for continuous control systems utilizing "bang-bang" control for which closed-form solutions for the probability densities are known. However, with discrete time and the closed-loop delay (of two intervals), standard analyses do not apply. We have instead resorted to simulation with the independent-increment driving function $(L_{r+1} - L_r)$ taken to be Gaussian (in decibels) with standard deviation σ, in accordance with the log-normal shadowing assumption. Note that the probabilities of up and down commands depend on the instantaneous $\overline{E}$ through (13) where F_C is a function of $\overline{E}$ as is evident from (1a) and the preceding definition of S, or (2a).

The results are shown in Fig. 4 for multipath-fading with $m = 1, 2$, and 4, as well as for the unfaded case. In each case, $N = 6$ and the standard deviation of the independent increments $L_r - L_{r-1}$ is taken to be 0.5 dB as is the energy increment Δ.

Also, in each instance, the probability that an up–down command is received incorrectly is taken to be $\gamma = 0.05$. The threshold ϕ in (11) and (15) is set so as to achieve a mean $\overline{E}/N_0 = 10$ dB, since by varying ϕ we may vary the mean of the distribution at will. It is noteworthy that the probability density of $\overline{E}/N_0$ does not differ much among the four cases.

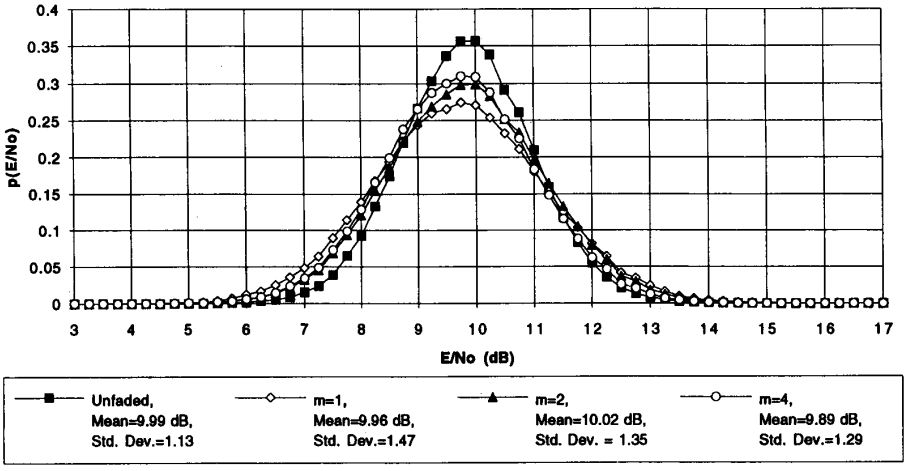

Fig. 4. Steady-state E_b/N_0 probability densities from simulation ($N = 6$, $M = 64$, gamma $= 0.05$).

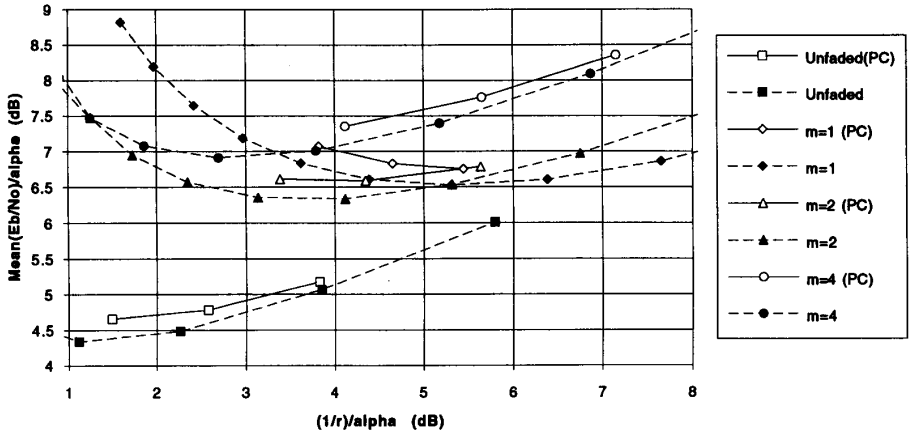

Fig. 5. Performance with integer metrics and power control in independent-increment lognormal fading (Std. Dev. = 0.5 dB).

It might be argued that the fading cases apply to very fast fading since the measurements are made on N successive (not interleaved) orthogonal signals and are assumed to be independent. On the other hand, the unfaded case could also be taken to be that for very slow fading where the energy remains constant over the N successive signal periods of the measurement, provided the time constant for the power control loop is much shorter than the bandwidth of the fading process. In the following, we shall take the power-controlled E_b/N_0 distribution in multipath to be that for fast fading in each case, which is a slightly pessimistic assumption since the corresponding standard deviation is somewhat larger than for the fixed energy case.

VI. Coded Error Performance with Ideal Interleaving and Power Control—Conclusions

Performance is determined by the relationship between $\overline{E}/N_0$ and r, through (6) and (7), which are both functions of Z. With integer metrics, Z is given by (10); but with the added effect of power control, each transition probability P_k, which depends on $\overline{E}$, must be replaced by its average.

$$\int_0^\infty P_k(\overline{E}/N_0)p(\overline{E}/N_0)d(\overline{E}/N_0), \qquad k = \pm 1, \cdots, 8 \tag{23}$$

where $P_k(\overline{E}/N_0)$ is given by (9a) and (9b) with $f_C(y)$ and $F_C(y)$ being functions of $\overline{E}/N_0$, and $p(\,)$ is the density function of the power-controlled $\overline{E}/N_0$, determined by simulation as shown in Fig. 4 for one choice of power control threshold ϕ.

Fig. 5 shows (as solid lines) the result of this calculation for the power-controlled case for three settings of power control thresholds ϕ for each of the faded and unfaded cases. Also shown as dotted lines are the corresponding values for fixed $\overline{E}_b/N_0$, as taken from Fig. 3. From this it is seen that power control degrades performance by less than 0.2 dB in each case.

It is also apparent from Fig. 5 that, $M = 64$, choosing a rate $1/3$ code with a backoff factor $\alpha = 0.8$ dB, as suggested in Appendix I to achieve $P_f < 0.01$, the resulting abscissa value for $(1/r)/\alpha$ is 4 dB. Then adding α to the corresponding ordinate values leads to mean $E_b/N_0 = 6.1$ dB for the unfaded

case and mean $\overline{E}_b/N_0 = 7.4$, 7.8, and 8.1 dB for $m = 1$-,2-, 4-path multipath.

Comparing with performance for optimum unquantized metrics (solid lines of Fig. 3), it is seen that the combined effect of quantization and power control degraded performance by no more than 0.6 dB. It should be emphasized in conclusion that all performance estimates were for the case of ideal interleaving between the encoder and the orthogonal waveform generator [Fig. 1(a)]. With finite interleaving, performance will generally degrade, particularly in fading which is slow relative to the interleaving span, but more rapid than the response time of the power control loop.

An additional advantage of power control not discussed in this paper is that since each user's power is individually controlled, users which are disadvantaged by excessive multipath, as well as greater range or shadowing, can be given additional power to achieve a higher E_b/N_0 ratio in excess of just what is required to equalize the received power for each user. Thus, power control affords the possibility of achieving a desired level of error probability for all users simply by varying E_b/N_0 requirements. This increased E_b/N_0 for selected users produces increased interference for other users, which ultimately limits the capacity of a given cell in terms of number of supportable users, as treated in [3]. However, when the total number of users is large, the number of disadvantaged users requiring higher E_b/N_0 ratios will to some extent be offset by the number enjoying favorable propagation and hence lower E_b/N_0 ratios. Thus, controlling power to achieve uniform error rates will on the average not severely impact average E_b/N_0 and, consequently, the interference suffered by the collection of users which governs the overall user capacity.

Appendix I
Generic and Specific Performance of Binary Convolutional Codes on Memoryless Channels

No digital communication system is complete without forward error control (FEC) coding. With wideband spread spectrum modulation, the coding redundancy is already present and consequently imposes no limitation on code rate. Moreover, FEC coding performance analysis is central to the design of the overall system; hence, a brief review of coding fundamentals is in order.

For any symmetric memoryless channel, characterized by interference and fading which is independent from symbol to symbol, there is a large number of binary convolutional codes with constraint length K and rate r bits/symbol for which the L-bit frame[5] error probability is upper bounded [7] by

$$P_f < \frac{L2^{-Kr_0/r}}{2\left[1 - 2^{-(r_0/r-1)}\right]}, \qquad r < r_0 \tag{A.1}$$

where the parameter r_0 is a function solely of the memoryless channel statistics given by

$$r_0 = 1 - \log_2(1 + Z) \tag{A.2}$$

[5]The frame or packet is assumed to contain $L - (K - 1)$ bits followed by $K - 1$ "flush tail" zeros.

where

$$Z = \int_{-\infty}^{\infty} \sqrt{p(y|x)p(y|\overline{x})}\, dy \tag{A.3}$$

with y being the channel (soft decision) output random variable and $x = 0$ or 1 and $\overline{x}$ its complement, being the binary channel inputs, with corresponding channel (conditional) transition probability density functions $p(y|x)$ and $p(y|\overline{x})$. Any channel can be converted into a memoryless channel by providing a sufficiently large symbol interleaver after the encoder and prior to modulation, and a corresponding deinterleaver after demodulation but before the decoder. Unfortunately, these generic upper bounds are relatively loose.

For a specific good convolutional code of constraint length K and rate r, a much tighter upper bound is provided by the expression [7]

$$P_f < \frac{L}{2} T(Z) \tag{A.4}$$

where $T(Z)$ is the code generating function and Z is given by (A.3). Based on the convergence region of the generic bound (A.1) and other theoretical considerations, r_0 is often considered a practical limit on the code rate r of the binary convolutional code. Hence, for a specific code of rate r and constraint length K whose P_f is bounded in terms of its generating function $T(Z)$, we may express the bound (A.4) in terms of r_0/r by using the inverse of (A.2),

$$Z = 2^{1-r}o - 1.$$

Thus, in Fig. 6, for the two codes of constraint length $K = 9$ and rates $1/2$ and $1/3$, whose shift register tap generators are, respectively, (753, 561) and (557, 663, 711) in octal notation, the frame error probability bound is shown as function of $\alpha = r_0/r > 1$ (in decibels). It appears that to achieve frame error rates below 10^{-2}, which is the acceptable level for vocoded voice traffic, $\alpha = 0.6$ dB for the $r = 1/2$ code, and $\alpha = 0.8$ dB for the $r = 1/3$ code[6].

Tighter bounds yet can be obtained, but these are more complex functions of all the memoryless channel transition probabilities and not just the r_0 parameter.

Appendix II
Performance of the Optimum M-ary Convolutional Codes Employing Interleaved-Orthogonal Signals

Consider a convolutional code which directly selects an M-ary orthogonal signal. Let b bits be shifted into the register to select n successive M-ary signals, where both b and n are integers. Hence, the code has rate $R = b/n$ bits/orthogonal signal and has 2^b branches emanating from each trellis node, with n orthogonal signals per branch. The generic L-bit frame error probability upper bound for a constraint length of bK bits is given by

$$P_f < \frac{L}{2}\left(\frac{2^b - 1}{b}\right)\frac{2^{-bKR_0/R}}{1 - 2^{-b[(R_0/R)-1]}} \tag{B.1}$$

[6]Even though it appears from this that the rate $1/2$ code is superior to the rate $1/3$ code for the same α, performance depends on the E_b/N_0 which is related to the r_0 parameter, as described above and shown in Fig. 3.

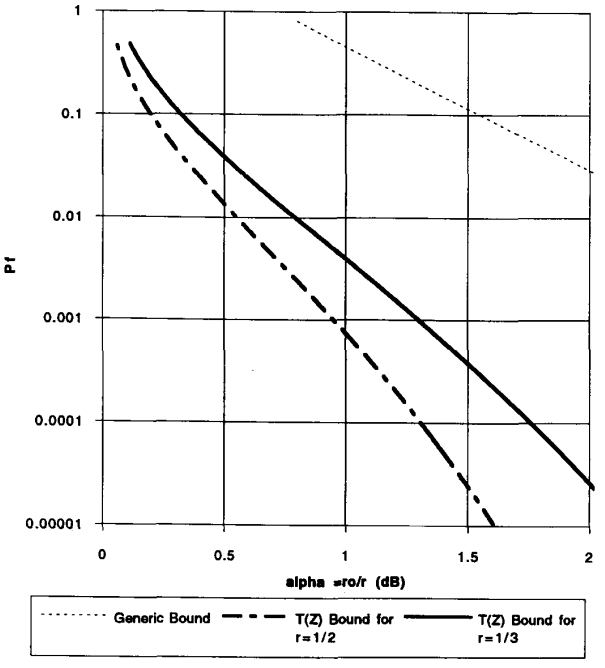

Fig. 6. Frame error probability bounds for $K = 9$, convolutional codes.

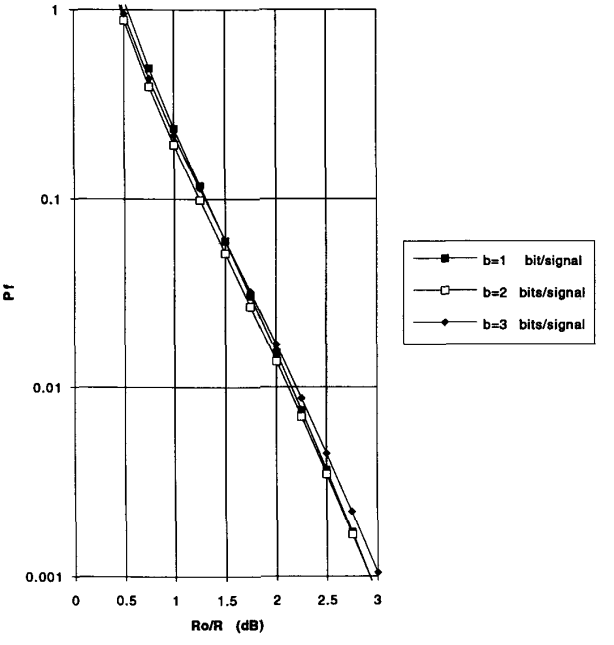

Fig. 7. Frame error rate as a function of Ro/R for $K = 9$ orthogonal convolutional codes.

where

$$R_0 = -\log_2\left(\frac{1}{M} + \frac{M-1}{M} Z\right) \tag{B.2}$$

and Z is the Chernoff (Bhattacharyya) bound for orthogonal signals. Note that here both R and R_0 can be greater than 1, while for $M = 2$, (B.2) reduces to (A.2).

However, if $M \geq 2^{bK}$, the generic bound becomes the specific bound for the orthogonal convolutional code, since in this case each of the 2^{bK} shift register tap combinations of the encoder can select a different orthogonal signal [4]. In this case, the bound (B.1) holds, but with[7]

$$R_0 = -\log_2 Z \tag{B.3}$$

or, equivalently, from (B.1) and (B.3)

$$P_f < \frac{L}{2}\left(\frac{2^b - 1}{b}\right)\frac{Z^{nK}}{1 - 2^b Z^n}.$$

Fig. 7 is a plot of the frame error rate bound (B.1) as a function of

$$\alpha = R_0/R \qquad \text{in decibels} \tag{B.4}$$

for $bK = 9$ and[8] $b = 1, 2$, and 3. It is noteworthy that the results are practically insensitive to the choice of b, but that to achieve $P_f < 10^{-2}$ requires $\alpha \approx 2$ dB.

[7]Obviously, this is also the limit of (B.2) as $M \to \infty$. In fact, (B.1) and (B.3) are closely approximated even for M as small as $2^{bK/2}$.

[8]While only $b = 1$ and $b = 3$ are consistent with $bK = 9$, we also include $b = 2$ in this comparison for completeness. A noninteger value of K could actually be implemented by puncturing a higher rate code.

To compare with the binary interleaved case, it is necessary to compute Z for orthogonal signals (which assumes the use of optimum likelihood function metrics),

$$Z = \iint \sqrt{p_a(y_a, y_b) p_b(y_a, y_b)}\, dy_a\, dy_b$$

where y_a and y_b are the envelope-matched filter outputs for any two branches that are compared by the decoder, with $p_a(y_a, y_b)$ being the joint probability of the two outputs when y_a corresponds to the correct decision, and conversely for $p_b(y_a, y_b)$. Thus, for the m-component multipath fading channel[9], since

$$p_a(y_a, y_b) = \frac{y_a^{m-1}}{(m-1)!}\,\frac{e^{-y_a/(1+S)}}{(1+S)^m} \cdot \frac{y_b^{m-1}}{(m-1)!}\, e^{-y_b}$$

and $p_b(y_a, y_b)$ is the same but with y_a and y_b interchanged,

$$\begin{aligned} Z &= \iint \frac{y_a^{m-1}}{(m-1)!}\,\frac{e^{-[y_a/(1+S)+y_a]/2}}{(1+S)^{m/2}}\,\frac{y_b^{m-1}}{(m-1)!} \\ &\quad \cdot \frac{e^{-[y_b/(1+S)+y_b]/2}}{(1+S)^{m/2}}\, dy_a\, dy_b \\ &= \frac{1}{(1+S)^m}\left[\int \frac{y^{m-1}}{(m-1)!} \exp\left[\frac{-y(1+S/2)}{1+S}\right] dy\right]^2 \\ &= \left[\frac{1+S}{(1+S/2)^2}\right]^m. \end{aligned} \tag{B.5}$$

[9]See also [8] for the derivation of (B.5).

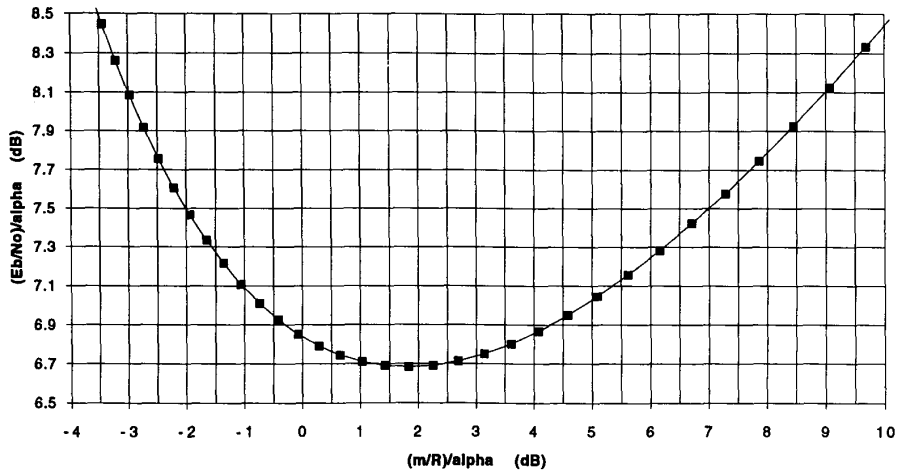

Fig. 8. Performance of optimum convolutional codes for interleaved orthogonal signals on M-path multipath fading channel.

Hence, from (B.3), we have that for orthogonal convolutional codes,

$$R_0 = -m \log_2 \left[\frac{1+S}{(1+S/2)^2} \right]. \tag{B.6}$$

Hence, using (B.4), we have

$$\frac{m/R}{\alpha} = \frac{m}{R_0} = -\frac{1}{\log_2 \left[\frac{1+S}{(1+S/2)^2} \right]} \tag{B.7}$$

and, using the definition of S,

$$\frac{\overline{E}_b/N_0}{\alpha} = \frac{Sm/R}{\alpha} = \frac{-S}{\log_2 \left[\frac{1+S}{(1+S/2)^2} \right]}. \tag{B.8}$$

From the parametric equations (B.7) and (B.8), $\overline{E}_b/N_0$ is obtained as a function of $(m/R/(\alpha))$ and plotted in Fig. 8.

From this it seems that it is possible to nearly optimize for both $m = 2$ and $m = 4$ multipath by choosing $b = n = R = 1$ bit /signal = 1 bit/branch. To achieve $P_f = 10^{-2}$, it is seen from Fig. 7 that $\alpha = 2$ dB. Then, for $m = 4$, $(m/R)/\alpha = 4$ dB, while for $m = 2$, $(m/R)/\alpha = 1$ dB, which implies from Fig. 8 that $(\overline{E}_b/N_0)/\alpha = 6.85$ dB and 6.7 dB, respectively and, hence, with ideal metrics,

$$\overline{E}_b/N_0 = 8.85 \text{ dB} \qquad \text{for } m = 4$$

and

$$\overline{E}_b/N_0 = 8.7 \text{ dB} \qquad \text{for } m = 2.$$

These appear to be more than 1 dB greater than the values of $\overline{E}_b/N_0$ required for a binary code with interleaving as shown in Fig. 3. Thus, even though for a given K, the code is optimum for the signal set, interleaving is performed only to the level of orthogonal signals, while with an interleaved binary code, interleaving is performed on binary symbols of which there are $\log_2 M$ as many. This implies that the greater diversity provided by ideal interleaving at the binary symbol level improves performance significantly over ideal interleaving only of the orthogonal signals.

REFERENCES

[1] G. L. Turin, "Introduction to spread-spectrum antimultipath techniques and their applications to urban digital radio," *Proc. IEEE,* vol. 68, pp. 328–353, Mar. 1980.
[2] J. Shapira, "Channel characteristics for the land cellular radio, and its system implications," submitted to *IEEE Trans. Antennas Propagat.*
[3] K. S. Gilhousen *et al.*, "On the capacity of a cellular CDMA system," *IEEE Trans. Vehicular Technol.*, vol. VT-40, pp. 303–312, May 1991.
[4] A. J. Viterbi, "Very low rate convolutional codes for maximum theoretical performance of spread-spectrum multiple-access channels," *IEEE J. Select. Areas Commun.*, vol. 8, pp. 641–649. May 1990.
[5] C. W. Helstrom, *Statistical Theory of Signal Detection,* 2nd ed. Oxford, UK: Pergamon, 1968.
[6] R. Price and P. E. Green, Jr., "A communication technique for multipath channels," *Proc. I.R.E.*, vol. 46, pp. 555–570, Mar. 1958.
[7] A. J. Viterbi, and J. K. Omura, *Principles of Digital Communication and Coding.* New York:McGraw-Hill, 1979.
[8] J. M. Wozencraft and I. M. Jacobs, *Principles of Communication Engineering.* New York:Wiley, 1965, Ch. 7.

Andrew J. Viterbi (S'54–M'58–SM'63–F'73) received the S.B. and S.M. degrees in electrical engineering from the Massachusetts Institute of Technology, Cambridge, in 1957, and the Ph.D. degree in electrical engineering from the University of Southern California, Los Angeles, in 1962.

He has devoted approximately equal segments of his career to academic research, industrial development, and entrepreneurial activities. In 1985 he was a cofounder and became Vice Chairman and Chief Technical Officer of QUALCOMM, Incorporated, a company specializing in satellite and terrestrial mobile communications. In 1968 he co-founded LINKABIT Corporation. He was Executive Vice President of LINKABIT from 1974 to 1982. In 1982 he took over as President of M/A-COM LINKABIT, Inc., and from 1984 to 1985 served as Chief Scientist and Senior Vice President of M/A-COM, Inc. Previously, from 1963 to 1973, he was a Professor at the UCLA School of Engineering and Applied Science, and from 1957 to 1962 he was a Research Engineer at C.I.T. Jet Propulsion Laboratory. He holds a part-time appointment as Professor of Electrical and Computer Engineering at the University of California, San Diego.

Dr. Viterbi has received numerous professional society awards and international recognition. These include three paper awards, culminating in the 1968 IEEE Information Theory Group Outstanding Paper Award, and four major society awards: the 1975 Christopher Columbus International Award (from the Italian National Research Council sponsored by the City of Genoa); the 1984 Alexander Graham Bell Medal (from IEEE sponsored by AT&T) "for exceptional contributions to the advancement of telecommunications," the 1990 Marconi International Fellowship Award and the 1992 NEC C&C Foundation Award (jointly). In 1991 he was awarded an Honorary Doctor of Engineering degree by the University of Waterloo, Ont., Canada. He is a member of the National Academy of Engineering.

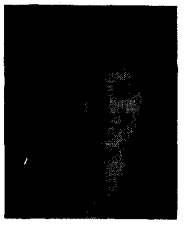

Audrey M. Viterbi (M'84) received the B.S. degree in electrical engineering and computer science and the B.A. degree in mathematics from the University of California, San Diego, in 1979. She received the M.S. and Ph.D. degrees in electrical Engineering from the University of California, Berkeley, in 1981 and 1985, repectively.

She was an Assistant Professor of Electrical and Computer Engineering at the University of California, Irvine, from 1985 to 1990. Since 1990 she has been at Qualcomm, Inc., San Diego, where she is currently a staff engineer involved in the development of the CDMA cellular telephone system. Her professional interests are in the area of modeling and performance evaluation of computer-communication networks and communications systems.

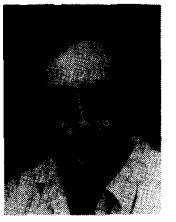

Ephraim Zehavi (M'77) received the B.Sc. and M.Sc. degrees in electrical engineering from the Technion–Israel Institute of Technology, Haifa, Israel, in 1977 and 1981, respectively, and the Ph.D. degree in electrical engineering from the University of Massachusetts, Amherst, in 1986.

From 1977 to 1983 he was an R&D Engineer and Group Leader in the Department of Communication, Rafael, Armament Development Authority Haifa, Israel. From 1983 to 1985 he was a Research Assistant in the Department of Electrical and Computer Engineering University of Massachusetts, Amherst. In 1985 he joined Qualcomm, Inc., San Diego, CA, as a Senior Engineer, where he was involved in the design and development of satellite communication systems, and VLSI design of Viterbi decoder chips. From 1988 to 1992 he was on the Faculty of Department of Electrical Engineering, Technion–Israel Institute of Technology, Haifa, Israel. He is currently a Principal Engineer at Qualcomm, Inc., working in the areas of satellite communication, digital cellular telephone systems, and combined modulation and coding.